Molecular Simulation, 2001, Vol. 27, pp. 99–114
Reprints available directly from the publisher
Photocopying permitted by license only

VAPOUR–LIQUID PHASE EQUILIBRIA OF *n*-ALKANES BY DIRECT MONTE CARLO SIMULATIONS

FLORENT GOUJON[a], PATRICE MALFREYT[a,*], ANNE BOUTIN[b] and ALAIN H. FUCHS[b]

[a]*Laboratoire de Thermodynamique des Solutions et des Polymères, UMR 6003 CNRS, Université Blaise Pascal, 63177 Aubière Cedex, France;*
[b]*Laboratoire de Chimie Physique, UMR 8000 CNRS, Université Paris-Sud, 91405 Orsay, France*

(Received November 2000; accepted November 2000)

We report results of direct Monte Carlo simulations of *n*-pentane and *n*-decane at the liquid–vapour interface for a number of temperatures. The intermolecular interactions are modeled using the last version of the anisotropic united atom model (AUA4). We have used the local long range correction energy and an algorithm allowing to select randomly with equal probability two different displacements. The liquid and vapour densities are in excellent agreement with experimental data and with those previously calculated using the GEMC method.

Keywords: Direct Monte Carlo simulations; Liquid–vapour equilibria; Explicit interface

1. INTRODUCTION

Knowledge of the phase behaviour of alkanes is essential for technological applications in the petrochemical industry. In the last decade, many computer simulations have been reported in the literature on the determination of phase equilibria. There have been significant theoretical efforts towards the simulation method and the potential models used for alkanes. Several different approaches have been developed to calculate the coexisting liquid and vapour densities. Among these methods, the Gibbs ensemble

*Corresponding author. e-mail: patrice.malfreyt@univ-bpclermont.fr

Monte Carlo technique (GEMC) [1–3] has been applied successfully to determine the vapour–liquid and liquid–liquid coexistence curves of molecular systems. Direct simulation using either Monte Carlo or molecular dynamics methods are the easiest methods for calculating phase equilibria but they are also computationally more expensive.

The Gibbs simulation technique simulates a system with two separate cells, each corresponding of the two corresponding phases. The conditions of phase equilibrium between the two phases are satisfied by moves of molecules in each phase, changes of the volume of the two phases and exchanges of molecules between the two phases. As a result, the coexisting densities can be calculated directly with a small total number of molecules. To enhance the sampling of hydrocarbon chains insertions at high densities, the Gibbs ensemble technique has been combined with the configurational bias Monte Carlo method [4–6]. Due to the fact that there is no physical contact between coexisting phases, this method cannot provide information about the interfacial properties.

The direct interfacial simulation method, which can be performed by Monte Carlo or molecular dynamics has been used successfully to study the liquid–vapour phase equilibria of several molecular fluids [7, 8]. The direct calculation of the two phases has not been widely applied to molecular systems because of the large number of molecules, the long equilibration times and the difficulty of estimating the long range corrections. In fact due to the nonuniform density distributions, the long range contribution are difficult to apply and are not considered in the most of previous simulations with explicit interface. Expressions of the long range corrections to the configurational energy of an inhomogeneous system have been developed by Guo *et al.* [9].

Ryckaert and Bellemans [10] were the first to implement the United Atom model (UA) in the simulations of n-alkanes. In this model, CH_3 and CH_2 groups are represented by single Lennard–Jones interaction sites. Different united atoms potentials have been developed and applied with good results to pure systems of alkanes. Siepmann *et al.* [11–13] have fitted parameters that allow a good prediction of the liquid–vapour phase equilibria and critical points of a large number of alkanes ranging from *n*-pentane (C_5) up to *n*-octatetracontane (C_{48}). The lack of explicit hydrogens becomes significant when we consider systems at high pressures where the hydrocarbons chains tend to pack together. Toxvaerd [14, 15] has introduced an anisotropic united atom potential (AUA) in which the interaction site is moved from being located directly on the original carbon atom site to the geometrical centre of the atoms that have been united

together. Delhommelle *et al.* [16] have studied the liquid–vapour coexistence curves for alkanes mixtures as a function of readjusted versions of the AUA model. Recently, a new parameterization AUA4 [17] of the AUA3 force field initially proposed by Toxvaerd [18] has shown better predictions of the critical temperature from coexistence density curves and of the equilibrium properties of pure *n*-alkanes in a large range of temperatures and hydrocarbon chain lengths.

The paper is organized as follows. In Section 2 of this paper, we present the latest version of the AUA potential with the intramolecular and intermolecular functions. Section 3 contains a description of the simulation technique used in this work. Section 4 deals with the simulation results for the *n*-pentane and *n*-decane and the comparison with the experimental values. We finish in Section 5 with the main conclusions of this work.

2. THE ANISOTROPIC UNITED ATOM MODEL (AUA)

In the United Atom (UA) model, the atom is represented by a spherical pseudo-atom with interaction site placed in the position of the carbon nucleus. In order to model the effects of hydrogen on the thermodynamic properties without increasing the number of interactions sites, Toxvaerd has introduced an Anisotropic United Atom Model (AUA). In this model, the interaction site is displaced from the carbon nucleus position to the geometrical centre of each united atom. In this case, the magnitude of the shift in the position of a site representing a CH_3 group is different to that for CH_2 group. In this work, we use the parameters of the AUA4 potential [17]. The distances of interaction site from carbon atom are: $d_1(CH_3) = 0.21584\,\text{Å}$ and $d_2(CH_2) = 0.38405\,\text{Å}$.

All united atoms on different molecules or separated by more three chemical bonds interact through a Lennard Jones potential:

$$u^{LJ}(r_{ij}) = 4\varepsilon_{ij}\left[\left(\frac{\sigma_{ij}}{r_{ij}}\right)^{12} - \left(\frac{\sigma_{ij}}{r_{ij}}\right)^{6}\right] \tag{1}$$

where ε_{ij} is the energy parameter of the interaction, σ_{ij} is the Lennard-Jones core diameter and r_{ij} is the distance between interactions sites i and j. The LJ parameters for the interactions between unlike atoms are calculated by using the Lorentz-Berthelot mixing rules:

$$\varepsilon_{ij} = (\varepsilon_{ii}\varepsilon_{jj})^{1/2} \quad \sigma_{ij} = \frac{1}{2}(\sigma_{ii} + \sigma_{jj}) \tag{2}$$

The interactions sites have the following Lenard-Jones parameters: $\varepsilon_{CH_3} = 120.15\,K$ and $\varepsilon_{CH_2} = 86.291\,K$. The size parameters are $\sigma_{CH_3} = 3.6072$ Å and $\sigma_{CH_2} = 3.4612$ Å.

In this AUA model version, the intramolecular interactions include contributions from bond angle bending interactions, torsional interactions and non-bonded interactions. The bond lengths are fixed to 1.535 Å. The bond angle potential has the following form,

$$u^{Bend} = \frac{1}{2} k_\theta (\cos\theta - \cos\theta_o)^2 \tag{3}$$

where θ is the angle between three consecutive united atoms, $k_\theta = 62500\,K$ is the bending angle, $\theta_o = 114°$ is the equilibrium bond angle.

The torsional potential function used is as follows,

$$u^{Tors} = \sum_{k=0}^{8} C_k \cos^k(\phi) \tag{4}$$

where ϕ is the dihedral angle between four subsequent united atoms, $C_0 = 1001.35\,K$, $C_1 = 2129.52\,K$, $C_2 = -303.06\,K$, $C_3 = -3612.27\,K$, $C_4 = 2226.71\,K$, $C_5 = 1965.93\,K$, $C_6 = -4489.34\,K$, $C_7 = -1736.22\,K$ and $C_8 = 2817.37\,K$.

As above-mentioned, the intramolecular non bonded interactions are represented by the Lennard-Jones function with the same potential parameters as used for the corresponding intermolecular potentials.

3. SIMULATION DETAILS

The simulations have been carried out in the NVT ensemble in a rectangular parallelepiped box of dimensions $L_x L_y L_z$ ($L_x = L_y$) with periodic conditions in all the directions. Intermolecular interactions have been computed to a certain cutoff r_c. The details of the simulations are summarized in Table I. The simulations have been performed in cycles. Each cycle consists of N randomly selected Monte Carlo moves with fixed probabilities, N being equal to the total number of molecules. The Monte Carlo moves we perform

TABLE I Number of alkanes molecules, box dimensions, cutoff value

System	*N*	*Lx/Å*	*Ly/Å*	*Lz/Å*	r_c/Å
C_5H_{12}	300	30.5	30.5	204	12.0
$C_{10}H_{22}$	250	33.1	33.1	240	15.0

are (1) displacement of a random molecule, (2) rotation of a randomly selected molecule around its centre of mass, (3) regrowing of part of random molecule using the configurational-bias scheme. As concerned the simulations of pentane, the relatives probabilities with which trial moves are attempted are set to 45% for the displacement, 35% for the rotation and 20% for the change of the internal configuration of a molecule. These probabilities are a little modified for the decane and are fixed to 40% (displacement), 30% (rotation), 30% (modification of the internal geometry). Thus, the maximum displacement and maximum rotation are adjusted during the equilibration phase to give an acceptance ratio of 0.4. For the modification of the conformation of a molecule, we use the configurational bias Monte Carlo technique which was adjusted to the AUA model by Smit *et al.* [11]. In this technique, we select randomly a molecule and the number of atoms to be regrown. The number of trial orientations range from 5 for C_5 to 6 for C_{10}. Using this procedure, we have obtained an acceptance probability for the modification of the internal structure which range from 35% at $T = 350\,K$ to 45% at $T = 425\,K$ for pentane and from 21% at $T = 450\,K$ to 31% at $T = 550\,K$ for decane. As concerned the translational moves, we have also tested an algorithm allowing to use randomly with equal probability two different maximum displacements. The two maximum displacements are adjusted separately during the equilibration phase to give acceptance ratios of 30% and 50%, respectively. The final acceptance ratio for the translational move is kept to 40%. This procedure should improve the sampling of the configuration space of the vapour phase by allowing larger displacements. A Verlet neighbour list is implemented in the code using a list sphere radius r_l depending of the type of moves. The difference value $(r_l - r_c)$ is equal to 2.0 Å for the translational move, to 5.5 Å (pentane) and 10.0 Å (decane) for the rotational move and to 12.5 Å (pentane) and 25.0 Å (decane) for the internal configurational change. These values result from several tests and lead to an efficient use of the Verlet list. As concerned the rotational move, 5.5 Å and 10 Å corresponds to the length of an unfolded molecule of pentane and decane, respectively. For the modification of the internal geometry, these values represent approximately two times the length of unfolded molecules. In a Monte Carlo simulation, the Verlet list must contain for each atom all the neighbours for which the pair distance is within r_l. This list of each atom is updated before each move of its corresponding molecule. As concerned the simulation of decane, the use of Verlet list yields gains in speed of about 30%.

In most of the previous simulations of inhomogeneous system, the long range corrections were not considered because of the difficulty of their

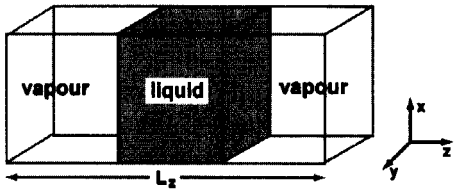

FIGURE 1 A parallelepiped box with a liquid phase surrounded on each side by a vapour phase. The z axis is perpendicular to the interface.

estimation due to the nonuniform density distribution. When the Lennard-Jones potential function is used for the nonbonded interaction, the total long range correction for the energy can be calculated analytically to give

$$U_{lrc} = \frac{8\pi}{3}\rho^2\sigma^3\varepsilon V\left[1/3\left(\frac{\sigma}{r_c}\right)^9 - \left(\frac{\sigma}{r_c}\right)^3\right] \tag{5}$$

where V is the volume of the simulation box and ρ the density. If the cell is divided into N_s slabs of width Δz, the total long range correction energy U_{lrc} can be calculated in terms of the local values u_{lrc} as follows

$$U_{lrc} = \sum_{k=1}^{N_s} u_{lrc}(k) \tag{6}$$

where $u_{lrc}(k)$ is the long range correction energy of the slab k. Guo *et al.* [9] have shown that the long range correction to configurational energy could be divided in two parts. An analytical solution is obtained for the first part

$$U_{lrc}^{(1)}(z_k) = \frac{8\pi}{3}\rho_k^2\sigma^3\varepsilon V_s\left[1/3\left(\frac{\sigma}{r_c}\right)^9 - \left(\frac{\sigma}{r_c}\right)^3\right] \tag{7}$$

where ρ_k and V_s are respectively the density and the volume of the slab k. The second part is expressed by

$$U_{lrc}^{(2)}(z_k) = \pi\rho_k V_s \int_{r_c}^{\infty} u(r)dr \int_{-r}^{r} \sum_{i=1}^{m} (\rho_i - \rho_{i-1})\, d\Delta z \tag{8}$$

It has been shown [9] that the second part is time-consuming and has only a minor contribution to the total long range energy. As a consequence, only the first part of the long range correction energy is included here in the total configurational energy. The long range correction energy of each slab is calculated after each move of molecular position.

The initial configuration has been generated by placing N alkane chains in a cubic box with random positions and by avoiding direct overlap with the molecules. An NpT Monte Carlo simulation has been performed over 20000 cycles on this bulk fluid configuration. The resulting box has been surrounded by two empty cells in the z direction. A typical run for a given temperature consisted of 20000 cycles ($6 \cdot 10^6$ moves) for equilibration followed by a production phase of additional 30000 cycles ($9 \cdot 10^6$ moves) where thermodynamic and structural quantities were collected. The equilibrated configuration was then used as the starting configuration for the next higher temperature. This procedure was repeated up to the highest temperature.

4. RESULTS AND DISCUSSIONS

We have tested different types of simulations on pentane. Firstly, we have achieved simulations without applying long range corrections to the total configurational energy. A second type of simulation has been performed using a standard constant tail correction. The third type of simulation divides the box into slabs and uses a local long range correction energy contribution for each slab. In this last one, we have also implemented an algorithm allowing to choose randomly two different displacements for a better exploration of the vapour phase. As concerned the simulation of *n*-pentane, the first maximum displacement Δr_1 value selected with a probability 0.3 increases from 0.54 Å (T = 350 K) to 1.21 Å (T = 425 K) whereas the second maximum displacement Δr_2 chosen with a probability 0.5 increases from 0.33 (T = 350 K) to 0.62 (T = 425 K). Compared with a simulation of *n*-pentane with only one displacement, the magnitude of the displacement value increases from 0.54 Å to 0.86 Å.

The Figure 2 displays the profiles of the long range corrections to the configurational energy along the z-axis for the *n*-pentane at four different temperatures. As an example, the standard uniform tail correction to the total energy is given in this plot. The contribution of the tail energy depends of the local density and increases therefore in the liquid region as the temperature is increased. The incorporation of the local long range corrections affects substantially the coexisting densities by increasing the liquid equilibrium densities. The combination of the local tail energies and of the two displacements improves the agreement of the calculated densities with the experimental values [19]. In fact, the deviation between experimental densities and simulated densities decreases from 2.3% to 0.9%

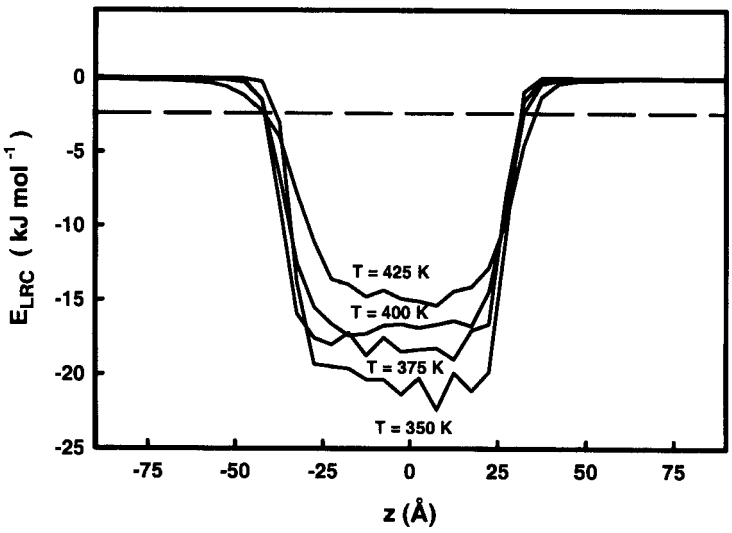

FIGURE 2 The long range corrections to the configurational energy (kJ mol^{-1}) along the z axis at four temperatures for *n*-pentane simulations. The dashed line represents a standard uniform correction to the total energy. The temperature is indicated in each case.

for the liquid densities and from 8.4% to 6.2% for the vapour densities while the local long range corrections and the two displacements are applied.

The density profiles are calculated during the simulation at every cycle. The fluctuations in the coexisting densities are estimated using the variation in block average. The density profile is determined in a simulation by dividing the box into slabs of width $\Delta z = 0.20$ Å perpendicular to the z-axis and recording an histogram of the number of molecules at every cycle. The density profiles $\rho(z)$ are shown in Figure 3 for the two temperatures T = 350 K and T = 425 K for the pentane and in Figure 4 for the decane at T = 450 K and T = 550 K. The dashed curves result from the fit to the density profiles to Eq. (9). The density curves of the pentane exhibit two well defined interfaces with a region of bulk liquid varying from 45 Å to 35 Å as the temperature increases from 350 K to 425 K. In addition, the profiles are symmetrical about the centre of the box and allow therefore an accurate estimation of the coexisting densities. Figure 4 shows the coexisting densities liquid and vapour for decane. The liquid densities region extends over a region varying from 62 Å to 55 Å as the temperature increases from 450 K to 550 K.

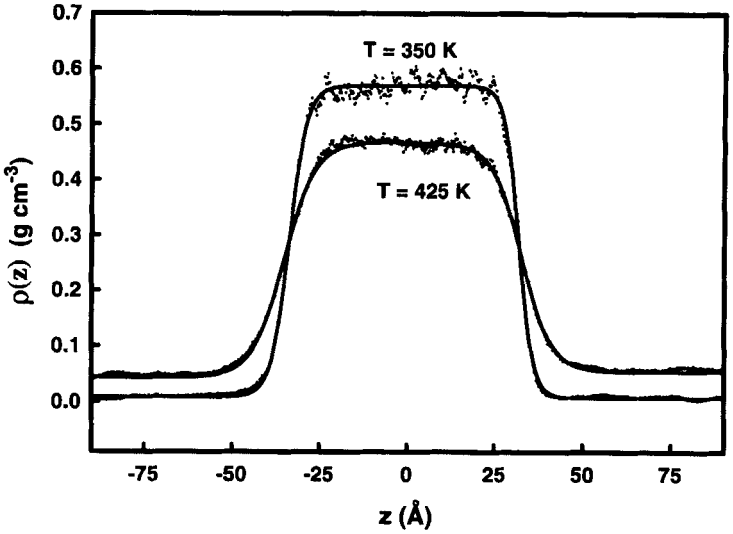

FIGURE 3 Density profiles for the two temperatures T = 350 K and T = 425 K for n-pentane. The continuous line are for the fitted tangent hyperbolic function. The temperature is indicated in each case.

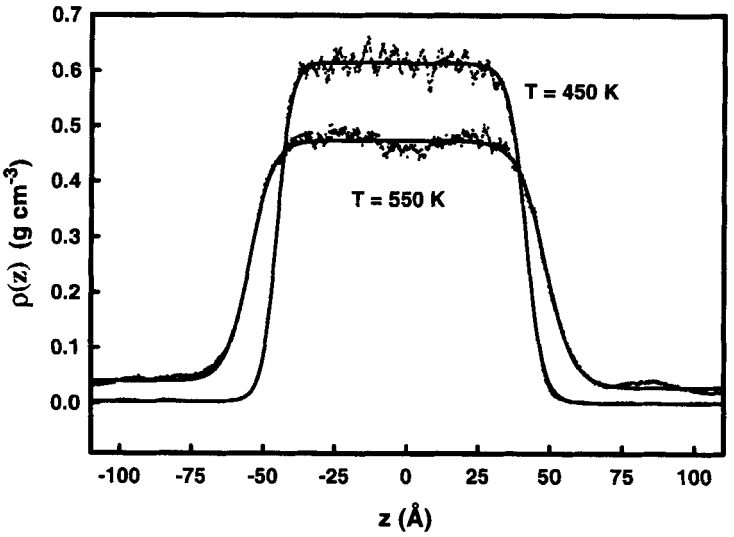

FIGURE 4 Density profiles for the two temperatures T = 450 K and T = 550 K for n-decane. The continuous line are for the fitted tangent hyperbolic function. The temperature is indicated in each case.

The coexisting densities in the bulk phases are obtained by fitting the simulated density profiles to a hyperbolic tangent function of the form:

$$\rho(z) = \frac{1}{2}(\rho_l + \rho_v) - \frac{1}{2}(\rho_l - \rho_v)\tanh\left(\frac{z - z_o}{d}\right) \tag{9}$$

In Eq. (9), ρ_l and ρ_v are the coexisting densities of the liquid and vapour phases, z_o is the position of the Gibbs dividing surface and d an approximate measure of the thickness of the interface. The Table II gives the liquid and vapour equilibrium densities and a measure of the thickness of the interface for *n*-pentane and *n*-decane. With increasing temperature, we observe that the width of the interface increases from 4.8 Å to 8.8 Å for pentane and 5.5 Å to 9.1 Å for decane. According to the root mean squared radius of gyration computed values (2.5 Å for pentane and 4.4 Å for decane), we estimate that the thickness of the interface corresponds roughly to 2 or 3 molecular layers for *n*-pentane and to 1 or 2 molecular layers for *n*-decane. The simulated coexisting densities are shown in Figure 5 for pentane and in Figure 6 for decane. In these figures, are included the coexisting densities of *n*-pentane and *n*-decane computed by GEMC method with the (AUA4) potential [16]. We can check that the agreement of the coexistence densities of this work with the corresponding experimental values and with the GEMC results is very satisfactory. In the case of *n*-pentane, density of the liquid phase is predicted with a deviation of about 1% whereas density is predicted in the gas phase with a deviation of less than 7%. As concerned the *n*-decane, the simulated liquid densities agree with the experimental data to within 3%. Larger deviations from experiment are observed for the vapour densities which are in most cases underestimated. The critical point [20] (T_c and ρ_c) is

TABLE II Simulation results for *n*-pentane and *n*-decane systems. The coexisting densities and the thickness of the interface d are reported. The subscript indicates the accuracy of the last decimal(s). The number 0.0815_{30} means 0.0815 ± 0.0030

	T/K	$\rho_l/g\,cm^{-3}$	$\rho_v/g\,cm^{-3}$	$d/Å$
C_5 pentane	350	0.569_9	0.008_2	4.8_8
	375	0.533_{13}	0.012_6	5.4_6
	400	0.503_{16}	0.025_9	6.5_{15}
	425	0.456_{27}	0.040_{14}	8.8_{22}
C_{10} decane	450	0.614_9	0.003_2	5.5_{10}
	475	0.585_{12}	0.008_6	5.7_7
	500	0.552_{12}	0.015_5	7.2_{18}
	525	0.518_{16}	0.020_4	8.1_{16}
	550	0.474_{21}	0.034_7	9.1_{30}

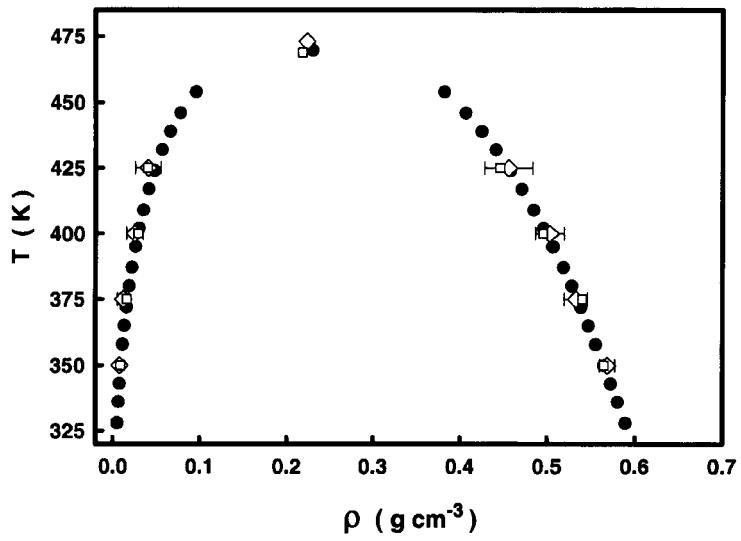

FIGURE 5 Vapour–liquid coexistence density curve of *n*-pentane computed with the direct method (◇), with the GEMC method (□) [17] compared with experimental data (•) [19]. The estimated critical point is also included in the curve.

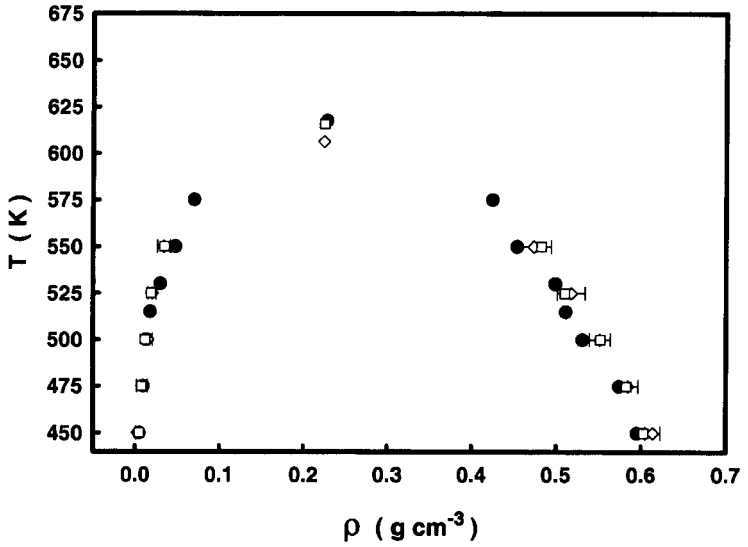

FIGURE 6 Vapour–liquid coexistence density curve of n-decane computed with the direct method (◇), with the GEMC method (□) [17] compared with experimental data (•) [19]. The estimated critical point is also included in the curve.

calculated by fitting the simulated coexistence densities to the law of rectilinear diameters

$$\frac{\rho_l + \rho_v}{2} = \rho_c + A(T - T_c) \tag{10}$$

and to the scaling law for the densities using an Ising-type critical exponent of $\beta = 0.32$

$$\rho_l - \rho_v = B(T - T_c)^{\beta} \tag{11}$$

The critical points of pentane and decane are given in Table III. We can observe that our simulations yield good predictions of the critical temperatures of pentane and decane which are within 1.5% of experiment. The critical densities seem to be a little underestimated but agree within for a maximum of 2.6% with the experimental data.

Figure 7 displays the centre of mass, the atomic and ends groups density profiles for decane at T = 300 K. The centre of mass and atomic density profiles are divided by the molecular mass to allow a better comparison between the three distributions. The centre of mass distribution is strongly peaked at the point where the atomic density profiles start to decrease. The profile of the ends groups indicates that the outer region of the interface (towards the vapour phase) ($z > 12$ Å) is dominated by ends groups. The combination of both regions rich in middle of chains and in ends chains suggest that the molecule of decane adopts an energetically unfavorable conformation which Harris [7] has called "horseshoe" conformation in the region corresponding to the peak of centre of mass profile ($6\text{ Å} < z < 10\text{ Å}$). Additional information on the conformation at the interface can be deduced from the components of the squared radius of gyration which is defined as [21]:

$$R_g^2 = \frac{1}{M}\sum_{i=1}^{n} m_i\left[(x_i - x_{com})^2 + (y_i - y_{com})^2 + (z_i - z_{com})^2\right] \tag{12}$$

TABLE III Critical points of n-pentane and n-decane. The experimental data are from [19]. The calculated critical temperatures result from the fitting of the coexisting densities to the Eqs. (10) and (11)

		Exp.	*MC.*
n-pentane	T_c (K)	469.7	473.1
	ρ_c (g · cm^{-3})	0.230	0.224
n-decane	T_c (K)	617.5	606.0
	ρ_c (g · cm^{-3})	0.228	0.224

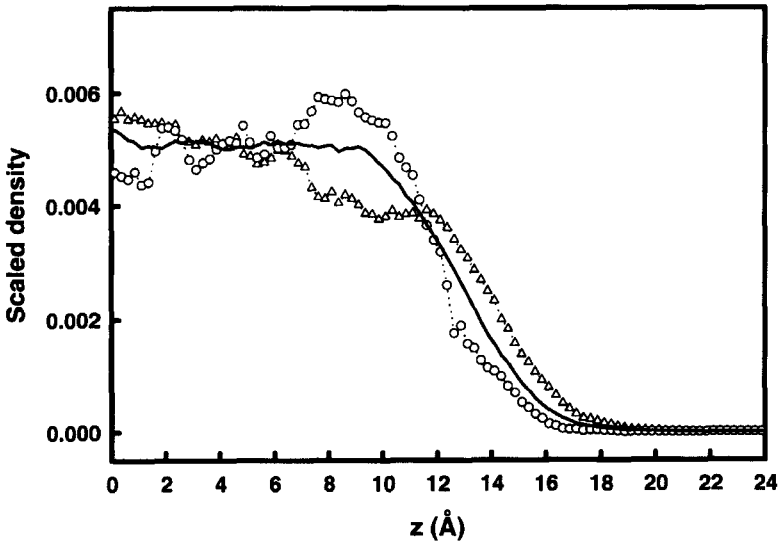

FIGURE 7 Scaled density profiles of the end atoms (△), centre of mass of the molecule (○) for *n*-decane at T = 300 K. The total hydrocarbon atoms profile is only represented by a solid line. The profiles of the total hydrocarbon atoms and of the centre of mass are divided by the molecular mass for clarity.

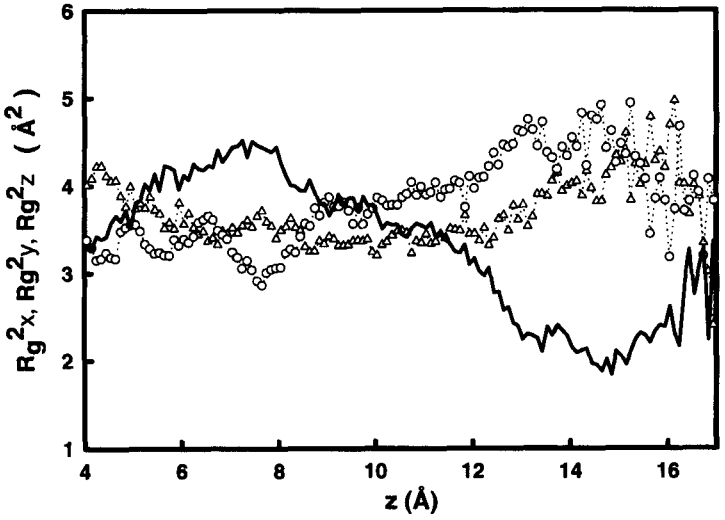

FIGURE 8 Components of the mean square radius of gyration of decane in x (△), y (○) directions as a function of the position of the centre of mass of *n*-decane at T = 300 K. The z component of the mean square radius of gyration is represented by a solid line.

where m_i is the mass of the united atom, M the molecular mass of decane, n the number of united atoms in the molecule and x_i, y_i and z_i are respectively the position of i atom along the x, y and z directions. The subscript "com" refers to the centre of mass of particular molecule. The distributions of the three components of the mean squared radius of gyration are displayed in Figure 8 as a function of the position of the centre of mass of each molecule. The components of the x and y directions in the region ($6\,\text{Å} < z < 10\,\text{Å}$) are smaller than the normal component to the interface. As concerned the region ($z > 12\,\text{Å}$) the normal component is significantly smaller than the x and y components. These show that the molecules of decane tend to align slightly parallel to the interface in the outermost region ($z > 12\,\text{Å}$) while they are slightly oriented perpendicular to the interface in the region corresponding to the peak of the centre of mass profile ($6\,\text{Å} < z < 10\,\text{Å}$). These structural and orientational features are in good agreement with those observed in a previous study [7]. These preferential structures and orientations as a function of the region are not detectable at higher temperatures.

5. CONCLUSIONS

We have demonstrated that the direct Monte Carlo simulations can be used to predict accurate liquid–vapour phase equilibria of moderately long alkane chains. We are aware of the system size dependence of the results. The simulated coexistence properties of the system studied in this work depend on a large number of parameters, *i.e.*, number of molecules, cutoff value, magnitude of the two displacements, local long range corrections to the energy, potential model. The set of parameters investigated in this paper has been successfully applied to produce accurate coexisting densities for *n*-pentane and *n*-decane that are in excellent agreement with experimental data and recent Gibbs Ensemble Monte Carlo results. The predictions of the critical properties are also in very good agreement with experiments.

The analysis of the components of the radius of gyration of *n*-decane at $T = 300\,\text{K}$ show that the decane molecule adopts two preferential orientations and conformations as a function of the distance from the interface. The conformation can be flattened and parallel to the interface towards the vapour phase and slightly elongated and perpendicular to the interface in the region beneath. The structural and orientational features do not occur at temperatures greater than 300 K.

An advantage of the direct Monte Carlo method over the GEMC method is that it should allow the study of long hydrocarbon chains by avoiding molecule insertions which are difficult at high densities. This renders the direct Monte Carlo method particularly adapted for the study of solid–liquid or solid–solid coexistence. In addition, the direct method provides information about the structure of the interface and can be used successfully to determine the surface tension. We are performing a work of this type to study the influence of the potential and of the cutoff radius on the surface tension.

Acknowledgment

The authors want to thank P. Ungerer for fruitful discussions about this work.

References

[1] Panagiotopoulos, A. Z. (1987). "Direct determination of phase coexistence properties of fluids by Monte Carlo simulation in a new ensemble", *Mol. Phys.*, **61**, 813.
[2] Panagiotopoulos, A. Z. (1992). "Direct determination of fluid phase equilibria by simulation in the Gibbs ensemble: a review", *Mol. Sim.*, **9**, 1.
[3] Panagiotopoulos, A. Z. (1995). "Gibbs ensemble techniques", in observation, prediction and simulation of phase transition in complex fluids, Rull, L. F., Baus, M. and Ryckaert, J. P., *NATO ASI ser. C*, **460**, 463.
[4] Rosenbluth, M. N. and Rosenbluth, A. W. (1955). "Monte Carlo calculations of the average extension of molecular chains", *J. Chem. Phys.*, **23**, 26.
[5] Frenkel, D., Mooij, G. C. A. M. and Smit, B. (1992). "Novel scheme to study structural and thermal properties of continuously deformable molecules", *J. Phys.: Condens. Matter*, **4**, 3053.
[6] de Pablo, J. J., Laso, J. J. and Suter, U. W. (1992). "Simulation of polyethylene above and below the melting point", *J. Chem. Phys.*, **96**, 2395.
[7] Harris, J. G. (1992). "Liquid vapor interfaces of alkane oligomers. Structure and thermodynamics from molecular dynamics simulations of chemically realistic models", *J. Phys. Chem.*, **96**, 5077.
[8] Alejandre, J., Tildesley, D. J. and Chapela, G. A. (1995). "Fluid phase equilibria using molecular dynamics: the surface tension of chlorine and hexane", *Mol. Phys.*, **85**, 651.
[9] Guo, M. and Lu, B. C. Y. (1997). "Long range corrections to thermodynamic properties of inhomogeneous systems with planar interfaces", *J. Chem. Phys.*, **106**, 3688.
[10] Ryckaert, J. P. and Bellemans, A. (1978). "Molecular dynamics of liquid alkanes", *Discuss. Faraday Soc.*, **66**, 95.
[11] Karaborni, S., Smit, B. and Siepmann, J. I. (1995). "Computer simulation of vapor–liquid phase equilibria of *n*-alkanes", *J. Chem. Phys.*, **102**, 2126.
[12] Siepmann, J. I., Karaborni, J. L. and Smit, B. (1993). "Simulating the critical behaviour of complex fluids", *Nature*, **365**, 330.
[13] Martin, M. G. and Siepmann, J. I. (1998). "Transferable potentials for phase equilibria. 1. United-Atom description of *n*-alkanes", *J. Phys. Chem. B*, **102**, 2569.
[14] Toxvaerd, S. (1990). "Molecular dynamics calculation of the equation of state of alkanes", *J. Chem. Phys.*, **93**, 4290.
[15] Padilla, P. and Toxvaerd, S. (1991). "Self-diffusion in n-alkane fluid models", *J. Chem. Phys.*, **94**, 5650.

[16] Delhommelle, J., Boutin, A., Tavitian, B., Mackie, A. D. and Fuchs, A. H. (1996). "Vapour–liquid coexistence curves of the united-atom and anisotropic united atom force fields for alkanes mixtures", *Mol. Phys.*, **96**, 1517.
[17] Ungerer, P., Beauvais, C., Delhommelle, J., Boutin, A., Rousseau, B. and Fuchs, A. H. (2000). "Optimization of the anisotropic united atoms intermolecular potential for *n*-alkanes", *J. Chem. Phys.*, **112**, 5499.
[18] Toxvaerd, S. (1997). "Molecular dynamics calculation of the equation of state of alkanes II", *J. Chem. Phys.*, **107**, 5197.
[19] Smith, B. D. and Srivastava, R. (1986). "*Thermodynamics of Pure Compounds: Hydrocarbons and Ketones*", Elsevier.
[20] Rowlinson, J. S. and Swinton, F. L. (1982). "*Liquid and Liquid Mixtures*", 3rd edn., London: Butterwoths.
[21] Doi, M. and Edwards, S. F. (1986). "*The Theory of Polymer Dynamics*", Clarendon Press: Oxford, UK.